# Impact of the MC-CDMA Physical Layer Algorithms on the Downlink Capacity in a Multi-Cellular Environment

Abdel-Majid MOURAD, Arnaud GUEGUEN, Ramesh PYNDIAH*
Mitsubishi Electric ITE, Telecommunications Research Laboratory, Rennes, France
* Ecole Nationale Supérieure des Télécommunications de Bretagne, Brest, France
{mourad, gueguen}@tcl.ite.mee.com

***Abstract* — This paper presents a methodology to evaluate the impact of the MC-CDMA physical layer algorithms on the downlink capacity in a multi-cellular environment. It presents a Monte Carlo simulation approach for capacity estimation at the system level and introduces a novel indicator for qualitative capacity evaluation at the link level. An illustration of this methodology shows very good agreement between the link level qualitative and system level quantitative capacity evaluations. The novel capacity indicator is therefore an efficient and accurate tool at the link level for optimizing the MC-CDMA physical layer algorithms and identifying the most appropriate physical layer configurations. On the other hand, the system level quantitative capacity evaluation allows to quantify more precisely the impact of the physical layer algorithms on the system capacity for a given environment.**

**Keywords – MC-CDMA, Capacity, Multi-Cell, Downlink.**

## I. INTRODUCTION

Two levels of study are required to account for the performance and design efficiency of a mobile radio communication system. The first level is referred to as the *link level*, while the second level is referred to as the *system level*. The link level study focuses on the quality of a single radio link between one transmitter and one receiver. Its main goal is to provide good abstraction of the quality of the various links that are jointly considered at the system level. This is achieved by establishing a mapping between the link performance typically measured in terms of the average bit (BER) and frame (FER) error rates, and an appropriate so-called link quality metric that should be accurate and easy to evaluate at both the link and system levels. The system level study however focuses on the performance of the global system made up of many active links jointly assessed by taking into account the system resources, the provided traffic services, and the deployment environment. The global system performance are typically evaluated in term of the system capacity, which reflects the maximum number of served users or the aggregate effective throughput [1].

The system capacity is estimated using a system level simulator within which several radio links are considered. Accurate capacity estimation ideally requires a time-driven or dynamic simulation approach that tries to simulate the real system behavior using accurate and realistic mobility and traffic models [2]. However, the main disadvantage of such approach lies in its large complexity and huge computational costs. A less complex approach not accounting for dynamic processes and referred to as the *Monte Carlo approach* has been extensively used in the literature for preliminary system level studies. This approach statistically estimates the system capacity by considering a large number of independent system realizations called *snapshots* [1]. This approach provides rough capacity estimates all the more as it does not account for the time evolution of the system. However, since it is simple and meaningful to perform preliminary system level analysis, we choose to adopt it here in this study.

Since there is no time dimension in the Monte Carlo approach, the maximum tolerated delay and minimum required effective throughput cannot therefore be considered as link quality requirements. The only remaining link quality requirement that can be considered is therefore the target FER. However, as the physical layer cannot be incorporated at the system level, the FER cannot therefore be measured online within the system level simulator. Observing a direct mapping between the signal to interference plus noise ratio (SINR) and FER, the SINR is commonly considered as an adequate link quality metric at the system level [1]. A target SINR required to achieve the target FER is derived from link level studies. This target SINR is specific to the given physical layer configuration and channel model, and thus, measuring the ability of the system to achieve the target SINR allows to reflect the impact of the physical layer on the whole system performance.

This study focuses on the impact of the MC-CDMA physical layer algorithms on the downlink system capacity, which we evaluate using a Monte Carlo system simulation approach. Favoring light mobile receiver design, we assume single user detection (SUD) based receiver algorithms. The SINR is taken here at the output of the SUD module, and thus it accounts for the detection algorithms. Moreover, the target SINR required to achieve the target FER for different MC-CDMA physical layer configurations is derived from the link to system level interface simulator presented in [6].

The rest of this paper is organized as follows. Section II briefly describes the MC-CDMA physical layer in the

downlink. Next, Section III presents the system model and the methodology adopted for evaluating the impact of the MC-CDMA physical layer on the downlink system capacity. Numerical results are then presented in Section IV, and finally, conclusions are drawn in Section V.

## II. MC-CDMA Physical Layer Description

Figure 1 depicts a block diagram of the MC-CDMA physical layer in the downlink (DL) [9].

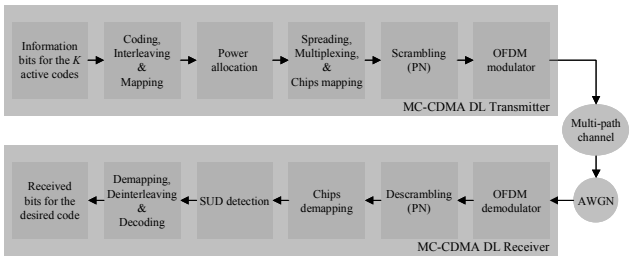


Figure 1. Block diagram of the DL MC-CDMA physical layer.

### A. MC-CDMA Downlink Transmitter

At the base station (BS) transmitter, the information bits of each active link are first encoded and bit interleaved, and then mapped to data symbols. After allocating the transmission powers for the active links, the data symbols of each link are spread with its assigned Walsh-Hadamard spreading code [7]. Next, chip-wise summation is performed over the chips of all links, and the resulting chips are then mapped to the time and frequency bins according to the chip mapping strategy. In the literature [7][8], two chip mappings are generally envisaged. The first mapping transmits the CDMA chips of one data symbol on independently faded sub-carriers, whereas the second mapping transmits the chips on highly correlated faded sub-carriers. It is clear that the first mapping provides higher frequency diversity than the second mapping to the detriment of higher multiple access interference (MAI). After chip mapping, the chips are chip-wise multiplied by a random subset of the BS pseudo-noise (PN) scrambling code in order to reduce the inter-cell interference. The scrambled chips are then sent to the OFDM modulator, which performs the IFFT operation and then inserts the guard interval. Next, the signal is sent through the multi-path channels of the active links.

### B. MC-CDMA Downlink Receiver

In addition to thermal noise, the signal received by the desired user is the summation of all the multi-user signals coming from all the BS. The maximum delay of all received signals is assumed smaller than the guard interval duration so that there is no inter-symbol interference. At the receiver side, the signal is first OFDM-demodulated by removing the guard interval and applying the FFT operation. Then, descrambling is performed, and the resulting chips are then demapped according to the chip mapping strategy employed by the transmitter. Next, single user detection (SUD) is performed in order to detect the desired signal. SUD detection consists in a chip-per-chip equalization followed by a despreading [7]. The typical equalization strategies that have been considered in the literature are [7][9]: equal gain combining (EGC), maximal ratio combining (MRC), and minimum mean square error combining (MMSEC). After SUD detection, the decision variables stream is first symbol demapped, and then deinterleaved and channel decoded in order to recover the transmitted binary information.

## III. Evaluation Methodology

### A. System Model

We consider an hexagonal regular macro-cellular system made up of one central cell surrounded by $N$ tiers of neighboring cells. The number of cells in the system is therefore equal to:

$$Q = 1 + 3N(N+1) \quad (1)$$

Figure 2 depicts the cellular layout with $N = 2$ tiers, which results in $Q = 19$ cells. Each cell has a centrally located BS fit with an omni-directional antenna. Each BS has at its disposal a maximum number of $M$ spreading codes, and its total output power is limited by $P_{max}$. For the sake of simplicity and in order to avoid the border effects [4], the results are collected only from the central cell although the whole system is simulated, and the $Q$-1 neighboring BS are assumed to transmit at the same fixed power $P_o \leq P_{max}$. The users are assumed uniformly distributed within the disk delimiting the hexagonal cells (cf. Figure 2). The connectivity between users and BS is performed following the minimum path loss criterion, i.e. a user is connected to the BS to which the path loss is minimum. A user is connected only to one BS, i.e. there is no handover, and all users are assumed to have the same physical layer configuration.

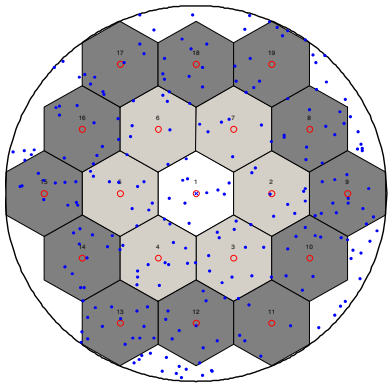

Figure 2. Cellular layout with $N = 2$ tiers and 250 users uniformly distributed within the disk delimiting the 19 hexagonal cells.

### B. Cellular Capacity Analysis

Let us consider the problem of satisfying the link quality requirements of the users connected to the central BS ($BS_1$). The link quality requirement is expressed in term of a target FER to achieve. Thanks to the direct SINR-FER mapping, the target FER can then be replaced by a target SINR. This target

SINR is derived from link level studies, and is specific to the given physical layer configuration and channel model. The problem of satisfying the SINR requirements under the constraint of limited BS power can then be formulated as:

$$\begin{aligned} &SINR_k = \lambda_\phi \quad \forall k = 1 \ldots K \le M \\ &p_k > 0 \quad P_c = \sum_{k=1}^{K} p_k \le P_{\max} \end{aligned} \tag{2}$$

where $\lambda_\phi$ denotes the target SINR that is specific to the physical layer configuration $\phi$. $K$ and $P_c$ are respectively the cell load and output power of $BS_1$, and $p_k$ is the power $BS_1$ should allocate to the $k$-th user in order to satisfy the SINR requirements. At last, $SINR_k$ denotes the local mean SINR at the output of the SUD module of the $k$-th user connected to $BS_1$, and it is given by [6]:

$$SINR_k = \frac{p_k g_{1k}}{g_{1k} \sum_{j=1, j\neq k}^{K} p_j \alpha_{kj} + \beta_k \left( \frac{1}{SF} \sum_{q=2}^{Q} P_o g_{qk} + P_n \right)} \tag{3}$$

where $g_{qk}$ stands for the path gain between $BS_q$ and the $k$-th user connected to $BS_1$. $\{\alpha_{kj}\}$ and $\beta_k$ are respectively the mutual intra-cell interference and inter-cell interference plus noise factors at the output of the SUD module. These factors are derived analytically in [6] from the equalized channel coefficients correlation and family of spreading codes. At last, $SF$ is the spreading factor and $P_n$ is the thermal noise power.

Making use of (3), (2) can be rewritten as the following power allocation problem for $BS_1$:

$$\begin{aligned} &\mathbf{p} = \lambda_\phi \left( \mathbf{A}\mathbf{p} + \mathbf{f} P_o + \mathbf{b} P_n \right) \\ &\mathbf{p} > \mathbf{0} \quad P_c = \mathbf{1}^T \mathbf{p} \le P_{\max} \end{aligned} \tag{4}$$

where $\mathbf{p}$ denotes the column vector of the $K$ powers $\{p_k\}$, $\mathbf{A}$ is a $K \times K$ matrix representing the intra-cell interference, and $\mathbf{f}$ and $\mathbf{b}$ are two column vectors of length $K$ representing respectively the inter-cell interference and thermal noise. $\mathbf{A}$, $\mathbf{f}$, and $\mathbf{b}$ are characterized by:

$$\begin{aligned} &A[k,j] = \alpha_{kj} \left( 1 - \delta_{kj} \right) \\ &f[k] = \frac{\beta_k}{SF} \sum_{q=2}^{Q} \frac{g_{qk}}{g_{1k}} \quad b[k] = \frac{\beta_k}{g_{1k}} \end{aligned} \tag{5}$$

where $\delta_{kj}$ stands for the Kronecker symbol that is equal to 1 for $k = j$, and 0 otherwise. The matrix $\mathbf{A}$ is not strictly positive since its diagonal is null, but it is regular, i.e. its square is strictly positive, and so the Perron-Frobenius theory applies [5]. It is well known from Perron-Frobenius theory for non negative matrices that the form $\mathbf{p} = \mathbf{A}\mathbf{p} + \mathbf{b}$ has a positive solution $\mathbf{p}^* = (\mathbf{I}-\mathbf{A})^{-1}\mathbf{b} > \mathbf{0}$ if and only if the maximum eigenvalue of $\mathbf{A}$ is strictly less than 1. Thus, the necessary and sufficient condition to obtain a positive and finite solution in (4) is that the maximum eigenvalue $\mu^*$ of $\mathbf{A}$ is less than $1/\lambda_\phi$. This condition is generally referred to as the *pole condition*, and the maximum cell load $K$ satisfying the pole condition is referred to as the *pole capacity* $K_{pole}$ [4]. The positive solution $\mathbf{p}^*$ in (4) can then be determined as:

$$\begin{aligned} &\mathbf{p}^* = \lambda_\phi \left( \mathbf{x} P_o + \mathbf{y} P_n \right) \\ &\mathbf{x} = \left( \mathbf{I} - \lambda_\phi \mathbf{A} \right)^{-1} \mathbf{f} \quad \mathbf{y} = \left( \mathbf{I} - \lambda_\phi \mathbf{A} \right)^{-1} \mathbf{b} \end{aligned} \tag{6}$$

By taking into account the constraint of limited BS power, we define the *constrained capacity* as:

$$K_{const} = \arg\max_{K} \left\{ \Pr\left( \mu^* > \frac{1}{\lambda_\phi} \bigcup P_c > P_{\max} \right) \le \varepsilon \right\} \tag{7}$$

where $\varepsilon$ denotes the maximum tolerated outage threshold typically set to 5%. The cell throughput can then be derived from (7) by multiplying $K_{const}$ by (1-FER)$R_\phi$, where $R_\phi$ is the single user bit rate for the physical layer configuration $\phi$.

### C. Capacity Indicator at the Link Level

Let us consider the case where $\alpha_{kj} \approx \alpha$ and $\beta_k \approx \beta$. In this case, the power $P_c = \mathbf{1}^T \mathbf{p}^*$ that is necessary to satisfy the SINR requirements can be simply written as (cf. (6)):

$$P_c = \frac{\lambda_\phi \beta K}{1 - \lambda_\phi (K-1)\alpha} T = C_\phi T \tag{8}$$

where:

$$T = \frac{1}{K} \sum_{k=1}^{K} \left( \frac{P_o}{SF} \sum_{q=2}^{Q} \frac{g_{qk}}{g_{1k}} + \frac{P_n}{g_{1k}} \right) \tag{9}$$

Note that $T$ in (9) is independent of the physical layer configuration $\phi$. Furthermore, by applying the law of large numbers to (9), $T$ can then be assumed independent of the cell load $K$. Only the factor $C_\phi$ in (8) remains therefore specific to the physical layer configuration $\phi$ and cell load $K$. Note that the factor $C_\phi$ needs only to be evaluated at the link level since it is only function of $\lambda_\phi$, $\alpha$, and $\beta$ (cf. (8)), which are outputs of the link to system level interface.

We extend the expression of the link level capacity indicator $C_\phi$ to the case of multiple factors $\{\alpha_{kj}\}$ as follows:

$$C_\phi = \frac{\lambda_\phi \beta K}{1 - \lambda_\phi \mu^*} \tag{10}$$

Thus, from (10), one can determine the maximum cell load $K_{max}$ at a given $C_\phi$ threshold. Note that the pole capacity can be simply determined from (10) as when $C_\phi$ tends to infinity.

The interest of this novel capacity indicator in (10) is that it allows to evaluate at the link level the impact of the physical layer algorithms on the system capacity, i.e. without performing system level simulations. This makes it an efficient and accurate tool at the link level for optimizing the physical layer algorithms and identifying the most appropriate physical layer configurations for a given environment.

### D. Particular Case of MMSEC Equalization

In the case of MMSEC equalization, the equalization coefficients are functions of the useful and interference

powers received by the $k$-th user [7]. The $n$-th equalization coefficient for the $n$-th channel coefficient $h[n]$ is given by:

$$w_k[n] = \frac{\sqrt{p_k g_{1k}}\,\overline{h}[n]}{\frac{P_c g_{1k}}{SF}|h[n]|^2 + \left(\frac{1}{SF}\sum_{q=2}^{Q} P_o g_{qk} + P_n\right)} \qquad (11)$$

Thus, in this case, the mutual intra-cell interference factors $\{\alpha_{kj}\}$ and inter-cell interference plus noise factors $\{\beta_k\}$, which are derived from the correlations of the equalized coefficients $\{h[n]w_k[n]\}$, become functions of the power vector $\mathbf{p}$. Thus, the power allocation problem in (4) becomes nonlinear as:

$$\mathbf{p} = \lambda_\phi\left(\mathbf{A}(\mathbf{p})\mathbf{p} + \mathbf{f}(\mathbf{p})P_o + \mathbf{b}(\mathbf{p})P_n\right) \qquad (12)$$

In order to find a solution to (12), the following recursive algorithm is proposed:

$$\mathbf{p}^{(r+1)} = \lambda_\phi\left(\mathbf{x}\left(\mathbf{p}^{(r)}\right)P_o + \mathbf{y}\left(\mathbf{p}^{(r)}\right)P_n\right) \quad \text{for } r = 1\ldots N_r \qquad (13)$$

where $r$ denotes the $r$-th recursion. It is observed that when (12) has a solution, the recursive algorithm in (13) converges to this solution in few ($N_r \le 5$) recursions for any positive and finite initial vector $\mathbf{p}^{(1)}$.

The factors $\{\alpha_{kj}\}$ and $\{\beta_k\}$ should therefore be evaluated online for each recursion for each snapshot within the system level simulator. This highly increases the computational costs since these factors require the computation of $K$ equalized channel coefficients correlations [6]. In order to reduce the computational costs, we make the following approximation:

$$w_k[n] \approx \sqrt{\frac{p_k}{g_{1k}}}\,v[n] \quad v[n] = \frac{\overline{h}[n]}{\frac{P_c}{SF}|h[n]|^2 + s} \qquad (14)$$

where $s$ replaces the second term in the denominator in (11) by its average over the $K$ users:

$$s = \frac{1}{K}\sum_{k=1}^{K}\left(\frac{P_o}{SF}\sum_{q=2}^{Q}\frac{g_{qk}}{g_{1k}} + \frac{P_n}{g_{1k}}\right) \qquad (15)$$

Thus, by using (14) instead of (11), only one correlation, i.e. that of the equalized coefficients $\{h[n]v[n]\}$, instead of $K$ correlations is therefore needed in order to evaluate the factors $\{\alpha_{kj}\}$ and $\{\beta_k\}$. This approximation has been validated via simulations where it is observed that using (14) instead of (11) increases the power $P_c$ only by less than 0.25 dBw. Thus, this approximation has negligible impact on the accuracy of the capacity estimates, however, it has the major advantage of significantly reducing the computational costs at the system level simulator.

At last, it is important to point out here that since the factors $\{\alpha_{kj}\}$ and $\{\beta_k\}$ are specific to each snapshot at the system level, the capacity indicator $C_\phi$, evoked in Section III.C for simple equalization schemes, becomes then specific to each snapshot. The exact value of $C_\phi$ cannot therefore be evaluated at the link level. However, one can still evaluate another $C_\phi$ at the link level by making use of the simplified link level MMSEC equalization coefficient given by [7]:

$$w[n] = \frac{\overline{h}[n]}{\frac{K}{SF}|h[n]|^2 + \sigma^2_{AWGN}} \qquad (16)$$

where $\sigma^2_{AWGN}$ is the variance characterizing the inter-cell interference plus noise at the link level. Thus, from (16), one can evaluate $C_\phi$ at the link level for different values of $\sigma^2_{AWGN}$.

## IV. Numerical Results

This section presents an illustration of the evaluation methodology presented in the previous section. It quantifies the impact of chip mapping strategies and equalization techniques on the system capacity in the context of the urban ETSI BRAN E channel model [10]. We consider six MC-CDMA physical layer configurations resulting from the combination of either adjacent (AFM) or interleaved (IFM) frequency domain chip mapping with either EGC, MRC, or MMSEC equalization. All the six configurations use the same modulation and coding scheme, which consists of QPSK-Gray modulation and UMTS-like convolutional code of rate ½. The key other parameters of the MC-CDMA physical layer are summarized in Table 1 [10].

| | |
|---|---|
| Sampling frequency $f_s$ | 57.6 MHz |
| FFT size $N_{fft}$ | 1024 |
| Guard interval size $N_g$ | 216 samples |
| Number of data carriers $N_c$ | 736 carriers |
| Frame size $N_f$ | 32 OFDM symbols |
| Spreading factor $SF$ | 32 |

Table 1. Key parameters of the MC-CDMA physical layer [10].

### A. Link Level Study

Table 2 summarizes the target SINR values required to achieve 1% target FER for all the six physical layer configurations. These values are obtained from the link to system level interface simulator in [6] for a cell load $K$ = 24. As discussed in [6], the target SINR is invariant with respect to $K$ in the IFM context, whereas in the AFM context, it is more or less invariant with respect to $K$ for $K$ in the range between 16 and 32. Thus, in the sequel, we confine our analysis to $K$ between 16 and 32.

| | **IFM context** | **AFM context** |
|---|---|---|
| **MRC** | 4.25 | 6.2 |
| **EGC** | 4.5 | 5.85 |
| **MMSEC** | 4.85 | 5.3 |

Table 2. Target SINR (dB) for 1% target FER.

Figure 3 illustrates the novel link level capacity indicator $C_\phi$ (cf. Section III.C) as a function of the cell load $K$ for all the six configurations. For MMSEC equalization, we consider two values of $\sigma^2_{AWGN}$ in (16): –5 and –10 dB.

From Figure 3, we can observe that for $K$ between 16 and 32, AFM-EGC outperforms IFM-EGC that in turn outperforms AFM-MRC and IFM-MRC. Moreover, IFM-MMSEC and AFM-MMSEC for both $\sigma^2_{AWGN}$ = -5 and -10 dB have very close performance to AFM-EGC. Thus, from this link level study, we conclude that AFM always outperforms IFM for any given equalization technique. Moreover, AFM-EGC, AFM-MMSEC, and IFM-MMSEC are similar and provide the highest system capacity.

### *B. System Level Study*

We consider the same standard large scale propagation model as in [4]. Table 3 summarizes the most relevant system level parameters [10].

| | |
|---|---|
| Number of tiers | $N = 2$ ($Q = 19$ cells) |
| Cell radius | 300 m |
| Thermal noise power density | -204 dBw/Hz |
| Propagation model | $l$ = -57.45 dB, $\delta$ = 2.8, $\sigma_s$ = 8 dB, $\rho$ = 0.5 |
| Number of codes at BS | $M$ = 32 codes |
| Outage threshold | $\varepsilon$ = 5 % |

Table 3. System level parameters.

Figure 4 depicts the pole capacity and the constrained capacity for $P_{max}$ = 13 dBw and $P_o$ = 3 and 6 dBw. As we can see from Figure 4, AFM always outperforms IFM for any given equalization. Moreover, AFM-EGC, AFM-MMSEC, and IFM-MMSEC are very close and provide the highest capacity. These results match very well those obtained from the previous analysis of the novel capacity indicator.

## V. CONCLUSIONS

This paper has presented a methodology to evaluate the impact of the MC-CDMA physical layer configurations on the downlink system capacity. This methodology allows to perform both qualitative and quantitative evaluations via link and system level analysis respectively. A very good match has been shown between qualitative evaluation using a novel link level capacity indicator and quantitative evaluation using a Monte Carlo system simulation approach. An illustration of this methodology has shown that in particular adjacent frequency domain chip mapping always outperforms interleaved mapping for any given equalization technique. This methodology can further be applied to quantify the impact on the system capacity of several MC-CDMA physical layer algorithms and configurations in different environments, which is crucial for system design.

## VI. REFERENCES


[1] J. Zander and S. L. Kim, "Radio Resource Management for Wireless Networks", *Artech House Publishers*, 2001.

[2] H. Holma, "A Study of UMTS Terrestrial Radio Access Performance", *Ph.D. dissertation, Helsinki University of Technology*, October 2003.

[3] ETSI Technical Report 101 112, "Selection Procedures for the Choice of Radio Transmission Technologies of UMTS", *UMTS 30.03, version 3.2.0*, 1998.

[4] N. Enderlé and X. Lagrange, "Analyse de la capacité descendante d'un système WCDMA", *Actes du congrès DNAC*, November 2001.

[5] E. Seneta, "Non-negative matrices and Markov chains", *Springer-Verlag*, second edition, 1981.

[6] A. Mourad et al., "Interface between Link and System Level Simulations for Downlink MC-CDMA Cellular Systems", *Proceedings of the 11th European Wireless Conference 2005*, Nicosia, April 2005.

[7] S. Hara and R. Prasad, "Design and Performance of Multi-carrier CDMA System in Frequency-Selective Rayleigh Fading Channels", *IEEE Transactions on Vehicular Technology*, Vol. 48, No. 5, September 1999.

[8] H. Atarashi et al., "Broadband Packet Wireless Access Based on VSF-OFCDM and MC/DS-CDMA", *IEEE PIMRC 2002*, Vol.3, September 2002.

[9] K. Fazel and S. Kaiser, "Multi-Carrier and Spread Spectrum Systems", *John Wiley & Sons Ltd*, 2003.

[10] IST-MATRICE, http://ist-matrice.org.


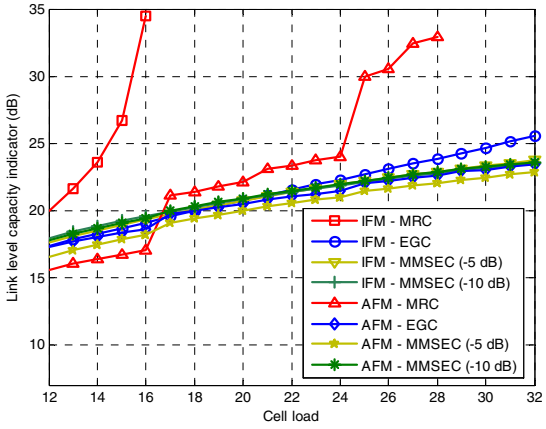


Figure 3. Link level capacity indicator (dB) versus the cell load.

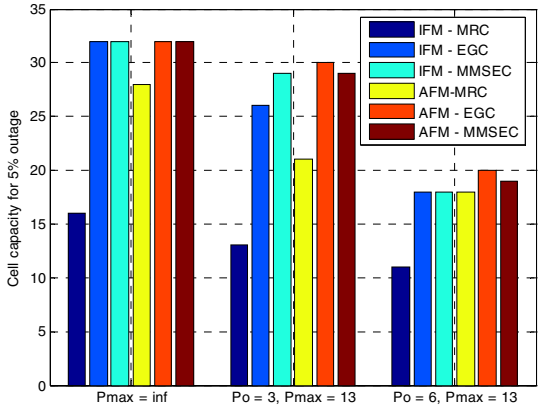


Figure 4. Pole and constrained capacity estimates.